

DESY 05-087
June 2005

ISSN 0418-9833

Search for Leptoquark Bosons in ep Collisions at HERA

H1 Collaboration

Abstract

A search for scalar and vector leptoquarks coupling to first generation fermions is performed using the e^+p and e^-p scattering data collected by the H1 experiment between 1994 and 2000. The data correspond to a total integrated luminosity of 117 pb^{-1} . No evidence for the direct or indirect production of such particles is found in data samples with a large transverse momentum final state electron or with large missing transverse momentum. Constraints on leptoquark models are established. For leptoquark couplings of electromagnetic strength, leptoquarks with masses up to $275 - 325\text{ GeV}$ are ruled out. These limits improve and supercede earlier H1 limits based on subsamples of the data used here.

(To be submitted to Phys. Lett. B)

A. Aktas¹⁰, V. Andreev²⁶, T. Anthonis⁴, S. Aplin¹⁰, A. Asmone³⁴, A. Astvatsaturov⁴,
A. Babaev²⁵, S. Backovic³¹, J. Bähr³⁹, A. Baghdasaryan³⁸, P. Baranov²⁶, E. Barrelet³⁰,
W. Bartel¹⁰, S. Baudrand²⁸, S. Baumgartner⁴⁰, J. Becker⁴¹, M. Beckingham¹⁰, O. Behnke¹³,
O. Behrendt⁷, A. Belousov²⁶, Ch. Berger¹, N. Berger⁴⁰, J.C. Bizot²⁸, M.-O. Boenig⁷,
V. Boudry²⁹, J. Bracinik²⁷, G. Brandt¹³, V. Brisson²⁸, D.P. Brown¹⁰, D. Bruncko¹⁶,
F.W. Büsser¹¹, A. Bunyatyan^{12,38}, G. Buschhorn²⁷, L. Bystritskaya²⁵, A.J. Campbell¹⁰,
S. Caron¹, F. Cassol-Brunner²², K. Cerny³³, V. Cerny^{16,47}, V. Chekelian²⁷, J.G. Contreras²³,
J.A. Coughlan⁵, B.E. Cox²¹, G. Cozzika⁹, J. Cvach³², J.B. Dainton¹⁸, W.D. Dau¹⁵,
K. Daum^{37,43}, Y. de Boer²⁵, B. Delcourt²⁸, A. De Roeck^{10,45}, K. Desch¹¹, E.A. De Wolf⁴,
C. Diaconu²², V. Dodonov¹², A. Dubak^{31,46}, G. Eckerlin¹⁰, V. Efremenko²⁵, S. Egli³⁶,
R. Eichler³⁶, F. Eisele¹³, M. Ellerbrock¹³, E. Elsen¹⁰, W. Erdmann⁴⁰, S. Essenov²⁵,
A. Falkewicz⁶, P.J.W. Faulkner³, L. Favart⁴, A. Fedotov²⁵, R. Felst¹⁰, J. Ferencei¹⁶, L. Finke¹¹,
M. Fleischer¹⁰, P. Fleischmann¹⁰, Y.H. Fleming¹⁰, G. Flucke¹⁰, A. Fomenko²⁶, I. Foresti⁴¹,
G. Franke¹⁰, T. Frisson²⁹, E. Gabathuler¹⁸, E. Garutti¹⁰, J. Gayler¹⁰, C. Gerlich¹³,
S. Ghazaryan³⁸, S. Ginzburgskaya²⁵, A. Glazov¹⁰, I. Glushkov³⁹, L. Goerlich⁶, M. Goettlich¹⁰,
N. Gogitidze²⁶, S. Gorbounov³⁹, C. Goyon²², C. Grab⁴⁰, T. Greenshaw¹⁸, M. Gregori¹⁹,
B.R. Grell¹⁰, G. Grindhammer²⁷, C. Gwilliam²¹, D. Haidt¹⁰, L. Hajduk⁶, M. Hansson²⁰,
G. Heinzelmann¹¹, R.C.W. Henderson¹⁷, H. Henschel³⁹, O. Henshaw³, G. Herrera²⁴,
M. Hildebrandt³⁶, K.H. Hiller³⁹, D. Hoffmann²², R. Horisberger³⁶, A. Hovhannisyan³⁸,
T. Hreus¹⁶, M. Ibbotson²¹, M. Ismail²¹, M. Jacquet²⁸, L. Janauschek²⁷, X. Janssen¹⁰,
V. Jemanov¹¹, L. Jönsson²⁰, D.P. Johnson⁴, A.W. Jung¹⁴, H. Jung^{20,10}, M. Kapichine⁸,
J. Katzy¹⁰, N. Keller⁴¹, I.R. Kenyon³, C. Kiesling²⁷, M. Klein³⁹, C. Kleinwort¹⁰,
T. Klimkovich¹⁰, T. Kluge¹⁰, G. Knies¹⁰, A. Knutsson²⁰, V. Korbel¹⁰, P. Kostka³⁹,
K. Krastev¹⁰, J. Kretzschmar³⁹, A. Kropivnitskaya²⁵, K. Krüger¹⁴, J. Kückens¹⁰,
M.P.J. Landon¹⁹, W. Lange³⁹, T. Laštovička^{39,33}, G. Laštovička-Medin³¹, P. Laycock¹⁸,
A. Lebedev²⁶, G. Leibenguth⁴⁰, B. Leißner¹, V. Lendermann¹⁴, S. Levonian¹⁰, L. Lindfeld⁴¹,
K. Lipka³⁹, A. Liptaj²⁷, B. List⁴⁰, E. Lobodzinska^{39,6}, N. Loktionova²⁶, R. Lopez-Fernandez¹⁰,
V. Lubimov²⁵, A.-I. Lucaci-Timoce¹⁰, H. Lueders¹¹, D. Lüke^{7,10}, T. Lux¹¹, L. Lytkin¹²,
A. Makankine⁸, N. Malden²¹, E. Malinovski²⁶, S. Mangano⁴⁰, P. Marage⁴, R. Marshall²¹,
M. Martisikova¹⁰, H.-U. Martyn¹, S.J. Maxfield¹⁸, D. Meer⁴⁰, A. Mehta¹⁸, K. Meier¹⁴,
A.B. Meyer¹¹, H. Meyer³⁷, J. Meyer¹⁰, S. Mikocki⁶, I. Milcewicz-Mika⁶, D. Milstead¹⁸,
D. Mladenov³⁵, A. Mohamed¹⁸, F. Moreau²⁹, A. Morozov⁸, J.V. Morris⁵, M.U. Mozer¹³,
K. Müller⁴¹, P. Murín^{16,44}, K. Nankov³⁵, B. Naroska¹¹, Th. Naumann³⁹, P.R. Newman³,
C. Niebuhr¹⁰, A. Nikiforov²⁷, D. Nikitin⁸, G. Nowak⁶, M. Nozicka³³, R. Oganezov³⁸,
B. Olivier³, J.E. Olsson¹⁰, S. Osman²⁰, D. Ozerov²⁵, V. Palichik⁸, I. Panagoulias¹⁰,
T. Papadopoulou¹⁰, C. Pascaud²⁸, G.D. Patel¹⁸, M. Peez²⁹, E. Perez⁹, D. Perez-Astudillo²³,
A. Perieanu¹⁰, A. Petrukhin²⁵, D. Pitzl¹⁰, R. Plačakyte²⁷, B. Portheault²⁸, B. Povh¹²,
P. Prideaux¹⁸, N. Raicevic³¹, P. Reimer³², A. Rimmer¹⁸, C. Risler¹⁰, E. Rizvi¹⁹, P. Robmann⁴¹,
B. Roland⁴, R. Roosen⁴, A. Rostovtsev²⁵, Z. Rurikova²⁷, S. Rusakov²⁶, F. Salvaire¹¹,
D.P.C. Sankey⁵, E. Sauvan²², S. Schätzel¹⁰, F.-P. Schilling¹⁰, S. Schmidt¹⁰, S. Schmitt¹⁰,
C. Schmitz⁴¹, L. Schoeffel⁹, A. Schöning⁴⁰, V. Schröder¹⁰, H.-C. Schultz-Coulon¹⁴,
K. Sedlák³², F. Sefkow¹⁰, R.N. Shaw-West³, I. Sheviakov²⁶, L.N. Shtarkov²⁶, T. Sloan¹⁷,
P. Smirnov²⁶, Y. Soloviev²⁶, D. South¹⁰, V. Spaskov⁸, A. Specka²⁹, B. Stella³⁴, J. Stiewe¹⁴,
I. Strauch¹⁰, U. Straumann⁴¹, V. Tchoulakov⁸, G. Thompson¹⁹, P.D. Thompson³, F. Tomasz¹⁴,
D. Traynor¹⁹, P. Truöl⁴¹, I. Tsakov³⁵, G. Tsipolitis^{10,42}, I. Tsurin¹⁰, J. Turnau⁶,
E. Tzamariudaki²⁷, M. Urban⁴¹, A. Usik²⁶, D. Utkin²⁵, S. Valkár³³, A. Valkárová³³,

C. Vallée²², P. Van Mechelen⁴, N. Van Remortel⁴, A. Vargas Trevino⁷, Y. Vazdik²⁶,
C. Veelken¹⁸, A. Vest¹, S. Vinokurova¹⁰, V. Volchinski³⁸, B. Vujicic²⁷, K. Wacker⁷,
J. Wagner¹⁰, G. Weber¹¹, R. Weber⁴⁰, D. Wegener⁷, C. Werner¹³, N. Werner⁴¹, M. Wessels¹⁰,
B. Wessling¹⁰, C. Wigmore³, Ch. Wissing⁷, R. Wolf¹³, E. Wünsch¹⁰, S. Xella⁴¹, W. Yan¹⁰,
V. Yeganov³⁸, J. Žáček³³, J. Zálešák³², Z. Zhang²⁸, A. Zhelezov²⁵, A. Zhokin²⁵, Y.C. Zhu¹⁰,
J. Zimmermann²⁷, T. Zimmermann⁴⁰, H. Zohrabyan³⁸ and F. Zomer²⁸

¹ *I. Physikalisches Institut der RWTH, Aachen, Germany*^a

² *III. Physikalisches Institut der RWTH, Aachen, Germany*^a

³ *School of Physics and Astronomy, University of Birmingham, Birmingham, UK*^b

⁴ *Inter-University Institute for High Energies ULB-VUB, Brussels; Universiteit Antwerpen, Antwerpen; Belgium*^c

⁵ *Rutherford Appleton Laboratory, Chilton, Didcot, UK*^b

⁶ *Institute for Nuclear Physics, Cracow, Poland*^d

⁷ *Institut für Physik, Universität Dortmund, Dortmund, Germany*^a

⁸ *Joint Institute for Nuclear Research, Dubna, Russia*

⁹ *CEA, DSM/DAPNIA, CE-Saclay, Gif-sur-Yvette, France*

¹⁰ *DESY, Hamburg, Germany*

¹¹ *Institut für Experimentalphysik, Universität Hamburg, Hamburg, Germany*^a

¹² *Max-Planck-Institut für Kernphysik, Heidelberg, Germany*

¹³ *Physikalisches Institut, Universität Heidelberg, Heidelberg, Germany*^a

¹⁴ *Kirchhoff-Institut für Physik, Universität Heidelberg, Heidelberg, Germany*^a

¹⁵ *Institut für Experimentelle und Angewandte Physik, Universität Kiel, Kiel, Germany*

¹⁶ *Institute of Experimental Physics, Slovak Academy of Sciences, Košice, Slovak Republic*^f

¹⁷ *Department of Physics, University of Lancaster, Lancaster, UK*^b

¹⁸ *Department of Physics, University of Liverpool, Liverpool, UK*^b

¹⁹ *Queen Mary and Westfield College, London, UK*^b

²⁰ *Physics Department, University of Lund, Lund, Sweden*^g

²¹ *Physics Department, University of Manchester, Manchester, UK*^b

²² *CPPM, CNRS/IN2P3 - Univ. Méditerranée, Marseille - France*

²³ *Departamento de Física Aplicada, CINVESTAV, Mérida, Yucatán, México*^k

²⁴ *Departamento de Física, CINVESTAV, México*^k

²⁵ *Institute for Theoretical and Experimental Physics, Moscow, Russia*^l

²⁶ *Lebedev Physical Institute, Moscow, Russia*^e

²⁷ *Max-Planck-Institut für Physik, München, Germany*

²⁸ *LAL, Université de Paris-Sud, IN2P3-CNRS, Orsay, France*

²⁹ *LLR, Ecole Polytechnique, IN2P3-CNRS, Palaiseau, France*

³⁰ *LPNHE, Universités Paris VI and VII, IN2P3-CNRS, Paris, France*

³¹ *Faculty of Science, University of Montenegro, Podgorica, Serbia and Montenegro*^e

³² *Institute of Physics, Academy of Sciences of the Czech Republic, Praha, Czech Republic*^{e,i}

³³ *Faculty of Mathematics and Physics, Charles University, Praha, Czech Republic*^{e,i}

³⁴ *Dipartimento di Fisica Università di Roma Tre and INFN Roma 3, Roma, Italy*

³⁵ *Institute for Nuclear Research and Nuclear Energy, Sofia, Bulgaria*^e

³⁶ *Paul Scherrer Institut, Villingen, Switzerland*

³⁷ *Fachbereich C, Universität Wuppertal, Wuppertal, Germany*

³⁸ *Yerevan Physics Institute, Yerevan, Armenia*

³⁹ DESY, Zeuthen, Germany

⁴⁰ Institut für Teilchenphysik, ETH, Zürich, Switzerland^j

⁴¹ Physik-Institut der Universität Zürich, Zürich, Switzerland^j

⁴² Also at Physics Department, National Technical University, Zografou Campus, GR-15773 Athens, Greece

⁴³ Also at Rechenzentrum, Universität Wuppertal, Wuppertal, Germany

⁴⁴ Also at University of P.J. Šafárik, Košice, Slovak Republic

⁴⁵ Also at CERN, Geneva, Switzerland

⁴⁶ Also at Max-Planck-Institut für Physik, München, Germany

⁴⁷ Also at Comenius University, Bratislava, Slovak Republic

^a Supported by the Bundesministerium für Bildung und Forschung, FRG, under contract numbers 05 H1 1GUA /1, 05 H1 1PAA /1, 05 H1 1PAB /9, 05 H1 1PEA /6, 05 H1 1VHA /7 and 05 H1 1VHB /5

^b Supported by the UK Particle Physics and Astronomy Research Council, and formerly by the UK Science and Engineering Research Council

^c Supported by FNRS-FWO-Vlaanderen, IISN-IIKW and IWT and by Interuniversity Attraction Poles Programme, Belgian Science Policy

^d Partially Supported by the Polish State Committee for Scientific Research, SPUB/DESY/P003/DZ 118/2003/2005

^e Supported by the Deutsche Forschungsgemeinschaft

^f Supported by VEGA SR grant no. 2/4067/24

^g Supported by the Swedish Natural Science Research Council

ⁱ Supported by the Ministry of Education of the Czech Republic under the projects INGO-LA116/2000 and LN00A006, by GAUK grant no 175/2000

^j Supported by the Swiss National Science Foundation

^k Supported by CONACYT, México, grant 400073-F

^l Partially Supported by Russian Foundation for Basic Research, grant no. 00-15-96584

Introduction

The ep collider HERA offers the unique possibility to search for the resonant production of new particles which couple directly to a lepton and a parton. Leptoquarks (LQs), colour triplet bosons which appear naturally in various unifying theories beyond the Standard Model (SM), are such an example. At HERA, leptoquarks could be singly produced by the fusion of the initial state lepton of energy 27.6 GeV with a quark from the incoming proton of energy up to 920 GeV.

The phenomenology of LQs at HERA is discussed in detail in [1]. The effective Lagrangian considered conserves lepton and baryon number, obeys the symmetries of the SM gauge groups $U(1)_Y$, $SU(2)_L$ and $SU(3)_C$ and includes both scalar and vector LQs. A dimensionless parameter λ defines the coupling at the lepton-quark-LQ vertex. At HERA, LQs can be resonantly produced in the s -channel or exchanged in the u -channel between the incoming lepton and a quark coming from the proton. In the s -channel, a LQ is produced at a mass $M = \sqrt{x s_{ep}}$ where x is the momentum fraction of the proton carried by the interacting quark.

This letter presents a search for LQs coupling to first generation fermions using e^+p data collected at a centre-of-mass energy of $\sqrt{s_{ep}} \approx 300$ GeV, e^-p data collected at $\sqrt{s_{ep}} \approx 320$ GeV and e^+p data collected at $\sqrt{s_{ep}} \approx 320$ GeV. These data sets correspond to integrated luminosities of 37 pb^{-1} , 15 pb^{-1} and 65 pb^{-1} respectively. They represent the full statistics accumulated by the H1 experiment between 1994 and 2000. The results of this search thus supercede those based on the e^+p 1994-1997 [1] and e^-p 1998-1999 [2] data.

The e^+p and e^-p data are largely complementary when searching for leptoquark resonances. Due to the more favourable parton densities of quarks with respect to anti-quarks at high x , the e^+p (e^-p) data sets are mostly sensitive to LQs with fermion number¹ $F = 0$ ($F = 2$). The search reported here considers the leptoquark decays into an electron and a quark and into a neutrino and a quark. These LQ decays lead to final states similar to those of deep-inelastic scattering (DIS) neutral current (NC) and charged current (CC) interactions at very high Q^2 , the negative four-momentum transfer squared. If the final state consists of an electron and a quark, the LQ mass is reconstructed from the measured kinematics of the scattered electron. If the final state consists of a neutrino and a quark, the LQ mass is reconstructed from the hadronic final state [1].

Neutral and Charged Current Data

The H1 detector components most relevant to this analysis are the liquid argon calorimeter, which measures the positions and energies of charged and neutral particles over the range $4^\circ < \theta < 154^\circ$ of polar angle², and the inner tracking detectors which measure the angles and momenta of charged particles over the range $7^\circ < \theta < 165^\circ$. A full description of the detector can be found in [3].

¹The fermion number F is given by $F = 3B + L$ with B and L being the baryon and lepton numbers respectively.

²The polar angle θ is defined with respect to the incident proton momentum vector (the positive z axis).

This search is based on inclusive NC and CC DIS data in the kinematic domain $Q^2 > 2500 \text{ GeV}^2$ and $0.1 < y < 0.9$, where the inelasticity variable y is defined as $y = Q^2/M^2$. The cuts on y remove regions of poor reconstruction, poor resolution, large QED radiative effects and background from photoproduction processes. The selection of NC-like events follows that presented in [1]. It requires an identified electron with transverse momentum above 15 GeV. The selection of CC-like events follows closely that presented in [1, 4]. A missing transverse momentum exceeding 25 GeV is required.

The inelasticity variable y is related to the polar angle θ^* of the decay lepton in the centre-of-mass frame of the hard subprocess ($eq \rightarrow lq$) by $y = \frac{1}{2}(1 + \cos \theta^*)$. Since the angular distribution of the electron coming from the decay of a scalar resonance is markedly different from that of the scattered lepton in NC DIS [1], a mass dependent cut on y was applied previously [1, 2] in order to optimise the signal sensitivity. However, the optimisation power is rather limited for a vector resonance as the angular distribution is only slightly different from that of the DIS background. For this reason, no such mass dependent y cut is applied in this analysis. Instead, all selected events are analysed in bins of varying size adapted to the experimental resolution in the $M - y$ plane, with a procedure designed to fully exploit the sensitivity to the signal as explained in the next section.

The mass spectra measured for NC- and CC-like events in the three data sets are compared in Figs. 1a-f with the SM predictions, obtained using a Monte-Carlo (MC) calculation [5] and the CTEQ5D parametrisation [6] for the parton densities. In all cases the data are well described by the SM prediction. Since no evidence for LQ production is observed in either the NC or CC data samples, the data are used to set constraints on LQs which couple to first generation fermions.

Statistical Method

For the limit analysis, the data are studied in bins in the $M - y$ plane. The binning used is different for the different data sets and is shown in Fig. 2. For those LQ types with only a NC-like decay mode, the total number of bins amounts to about 200 covering all three NC samples. The total number of bins doubles when including the three CC data samples for LQs having both NC-like and CC-like decay modes. The number of SM background events b_i in each bin i is obtained from the SM MC calculations. Each MC event k , reconstructed in bin i , has an event weight e_k , such that the MC is normalised to the luminosity of the data. The sum over all SM MC events within bin i thus gives

$$b_i = \sum_{k \in \text{bin } i} e_k. \quad (1)$$

To estimate the LQ signal, an event re-weighting technique is applied to the same SM MC events. No use is made of a dedicated signal MC generator. The number of events expected in each bin i in the presence of a LQ signal is denoted as $s_i + b_i$. It may be written as

$$s_i + b_i = \sum_{k \in \text{bin } i} e_k \frac{\sigma_k^{\text{LQ}} + \sigma_k^{\text{INT}} + \sigma_k^{\text{SM}}}{\sigma_k^{\text{SM}}}, \quad (2)$$

where $\sigma_k^{\text{LQ,INT,SM}}$ are differential cross section terms [7] corresponding to the LQ, interference and SM contributions, respectively. These differential cross section terms, calculated in leading order using the parton density functions CTEQ5D [6], are based on the true kinematic quantities of event k , whereas the resulting $s_i + b_i$ events are counted in the $M - y$ bins of the reconstructed variables with appropriate simulation of the detector response. The differential cross section terms $\sigma_k^{\text{LQ,INT}}$ depend on the LQ mass and coupling λ . For mass values well below the kinematic limit $\sqrt{s_{ep}}$, the s -channel contribution dominates in the LQ cross section and the signal contribution s_i to bin i is always positive. However, at higher masses, the interference contributions become more important and s_i may be negative in the case of destructive interferences, although $s_i + b_i$ always stays positive.

The limits are determined from a statistical analysis which uses the method of fractional event counting [8]. For a given leptoquark mass and coupling a weight w_i is ascribed to each bin, which is given by the asymmetry between the expected number of events in the presence or absence of a LQ signal:

$$w_i = \frac{(s_i + b_i) - b_i}{(s_i + b_i) + b_i} = \frac{s_i}{s_i + 2b_i}. \quad (3)$$

As an example, Fig. 2 illustrates the bin dependent weights for an e^+d type vector LQ having a mass of 200 GeV, a coupling of 0.023 and both the NC-like and CC-like decay channels. As expected, the weights are small for the e^-p data. For the e^+p data sets, the weights have little y -dependence.

Using these weights a fractional event count, also called test statistics, is defined as

$$X(\text{data}) = \sum_i w_i N_i(\text{data}), \quad (4)$$

where $N_i(\text{data})$ is the number of data events observed in bin i .

In a frequentist approach, a large number of “experiments” ($2 \times 10\,000$) are generated. Each experiment consists of Poisson distributed random numbers $N_i(b)$ ($N_i(s + b)$), based on the expected number of events b_i ($s_i + b_i$) in the absence (presence) of a LQ signal. For each background experiment b and for each signal-plus-background experiment $s + b$ a fractional event count is defined in analogy to Eqn.(4):

$$X(b) = \sum_i w_i N_i(b) \quad (5)$$

$$X(s + b) = \sum_i w_i N_i(s + b). \quad (6)$$

Frequentist probabilities CL_{s+b} (CL_b) are defined as the fraction of experiments where the quantity $X(s + b)$ ($X(b)$) is smaller than $X(\text{data})$. If the data agreed perfectly with the expectation from the background-only hypothesis, a value of $\text{CL}_b = 0.5$ would be obtained. A higher value indicates that the observation is more signal-like; a lower value indicates fluctuations opposite to those expected for a signal. If CL_{s+b} is small, it may be used to exclude the signal-plus-background hypothesis with confidence level $(1 - \text{CL}_{s+b})$. However, in this analysis we use the confidence level CL defined as

$$\text{CL} = 1 - \text{CL}_{s+b}/\text{CL}_b \quad (7)$$

to set limits in a conservative manner. This ratio, which was also used in LEP searches [8, 9], has the desirable feature that as the LQ coupling tends to zero, and necessarily $CL_{s+b} \rightarrow CL_b$, CL drops to 0, i.e. one cannot rule out any LQ which has a vanishing coupling. On the other hand, for a non-zero coupling, an exclusion limit at 95% CL is always reachable for a sufficiently large coupling.

Systematic uncertainties enter as offsets $\delta_{i,j}^b$ and $\delta_{i,j}^{s+b}$ to the predicted number of events b_i and $s_i + b_i$, where j runs over all independent sources of systematic errors. For the limits presented below, both the bin weights w_i and the b and $s + b$ MC experiments are altered by the known systematic uncertainties, assuming that the latter have Gaussian probability densities.

The experimental systematic error is dominated by the electromagnetic energy scale (between 0.7% and 3%) for the NC analysis, and by the hadronic energy scale (2%) for the CC analysis. The limited knowledge of proton structure causes an uncertainty on the signal cross section. This uncertainty is estimated to be 5% for $F = 2$ ($F = 0$) LQs coupling to e^-u (e^+u) and varies between 7% at low LQ masses up to 30% around 290 GeV for $F = 2$ ($F = 0$) LQs coupling to e^-d (e^+d). Similarly, an uncertainty on the DIS cross sections is connected with the parton densities. The correlation between the systematic uncertainties on the signal and that on the background and between different analysis bins is taken into account. The correlations induced by the uncertainties of the parton densities are evaluated using [10].

Limit Results

In the following limits will first be derived within the phenomenological model proposed by Buchmüller, Rückl and Wyler (BRW) [7] and then within generic models where the branching ratios β_e (β_ν) for the LQ decays into eq (νq) are not fixed.

The BRW model describes 7 LQs with $F = 0$ and 7 LQs with $F = 2$. We use here the nomenclature of [11] to label the various scalar $S_{I,L}$ ($\tilde{S}_{I,R}$) or vector $\tilde{V}_{I,L}$ ($V_{I,R}$) LQ types of weak isospin I , which couple to a left-handed (right-handed) electron. The tilde is used to distinguish LQs which differ only by their hypercharge. In the BRW model the branching ratios β_e (β_ν) are fixed and equal to 1 or 0.5 (0 or 0.5) depending on the LQ quantum numbers. Table 1 lists the 14 LQ types according to the BRW model.

For LQs with $F = 0$, the upper limits on the coupling obtained at 95% CL are shown as a function of the LQ mass in Figs. 3a and b, for scalar and vector LQs respectively. For masses above ~ 270 GeV, these bounds improve by a factor of up to ~ 3 the limits obtained in [1] from the analysis of e^+p data at $\sqrt{s_{ep}} = 300$ GeV. Constraints corresponding to $F = 2$ LQs are shown in Figs. 3c and d which extend those in [2] beyond the kinematic limit. For a coupling of electromagnetic strength α_{em} ($\lambda = \sqrt{4\pi\alpha_{\text{em}}} = 0.3$) this analysis rules out LQ masses below 275 to 325 GeV, depending on the LQ type.

Fig. 4 summarises the constraints on the $\tilde{S}_{1/2,L}$ and on the $S_{0,L}$ obtained by H1, by the OPAL and L3 experiments at LEP [12], and by the D0 experiment at the Tevatron [13]. The limits shown from LEP are from indirect constraints. The limits from the Tevatron are independent of the coupling λ as they were derived from the dominant pair production processes. The H1

$F = 2$	Prod./Decay	β_e	$F = 0$	Prod./Decay	β_e
Scalar Leptoquarks					
$S_{0,L}$	$e_L^- u_L \rightarrow e^- u$ $\rightarrow \nu d$	1/2 1/2	$S_{1/2,L}$	$e_R^+ u_R \rightarrow e^+ u$	1
$S_{0,R}$	$e_R^- u_R \rightarrow e^- u$	1	$S_{1/2,R}$	$e_L^+ u_L \rightarrow e^+ u$	1
$\tilde{S}_{0,R}$	$e_R^- d_R \rightarrow e^- d$	1		$e_L^+ d_L \rightarrow e^+ d$	1
$S_{1,L}$	$e_L^- d_L \rightarrow e^- d$ $e_L^- u_L \rightarrow e^- u$ $\rightarrow \nu d$	1 1/2 1/2	$\tilde{S}_{1/2,L}$	$e_R^+ d_R \rightarrow e^+ d$	1
Vector Leptoquarks					
$V_{1/2,R}$	$e_R^- d_L \rightarrow e^- d$	1	$V_{0,R}$	$e_L^+ d_R \rightarrow e^+ d$	1
	$e_R^- u_L \rightarrow e^- u$	1	$V_{0,L}$	$e_R^+ d_L \rightarrow e^+ d$ $\rightarrow \bar{\nu} u$	1/2 1/2
$V_{1/2,L}$	$e_L^- d_R \rightarrow e^- d$	1	$\tilde{V}_{0,R}$	$e_L^+ u_R \rightarrow e^+ u$	1
$\tilde{V}_{1/2,L}$	$e_L^- u_R \rightarrow e^- u$	1	$V_{1,L}$	$e_R^+ u_L \rightarrow e^+ u$ $e_R^+ d_L \rightarrow e^+ d$ $\rightarrow \bar{\nu} u$	1 1/2 1/2

Table 1: Leptoquark isospin families in the Buchmüller-Rückl-Wyler model. Charge conjugate processes are not shown. For each leptoquark, the subscript denotes its weak isospin. For simplicity, the leptoquarks are conventionally indexed with the chirality of the incoming *electron* which could allow their production in $e^- p$. The variable β_e denotes the branching ratio of the LQ into $e + q$.

limits are comparable with those from the ZEUS experiment obtained in a similar analysis [14]. The limits at high mass values are also compared with those obtained in a contact interaction analysis [15], which was based on the measured single differential cross sections $d\sigma/dQ^2$ from the NC process only [16].

Beyond the BRW ansatz, generic LQ models can also be considered. An example is provided by supersymmetric models³ where the R-parity is violated by a λ'_{1j1} (λ'_{11k}) coupling, with the \tilde{u}_L^j (\tilde{d}_R^{k*}) squark having the same interactions with a lepton-quark pair as the $\tilde{S}_{1/2,L}$ ($S_{0,L}$). In generic LQ models other LQ decay modes are allowed such that the branching ratios β_e and β_ν are free parameters. Mass dependent constraints on the LQ branching ratios can then be set for a given value of λ . For a vector LQ coupling to $e^+ d$ (possessing the quantum numbers of the $V_{0,L}$) and for $\lambda = 0.06$, a domain of the β_e - M (β_ν - M) plane can be excluded by the NC (CC) analysis as shown in Fig. 5a. If the LQ decays into eq or νq only⁴, the combination of both channels rules out the part of the plane on the left of the second full curve from the left for $\lambda = 0.06$. The resulting combined bound is largely independent of the individual values

³More general limits on squark production taking direct and indirect *R*-parity violating decay modes into account have been set in [17].

⁴It should be noted that $\beta_e + \beta_\nu = 1$ does not imply $\beta_e = \beta_\nu$ even when invariance under $SU(2)_L$ transformations is required. For example, when LQs belonging to a given isospin multiplet are not mass eigenstates, their mixing usually leads to different branching ratios in both channels for the physical LQ states.

of β_e and β_ν . Combined bounds are also shown for $\lambda = 0.03$ and $\lambda = 0.3$. For a coupling $\lambda = 0.3$ and high β_ν the limit extends to high mass values above the kinematic limit of resonant LQ production. For this part of the parameter space, the coupling $\lambda_\nu = \lambda\sqrt{\beta_\nu/\beta_e}$ is large⁵ but still satisfies $\lambda_\nu^2/4\pi < 1$. A smooth transition is observed between limits driven by resonant production and limits driven by contact interactions. Fig. 5b shows similar exclusion limits as for Fig. 5a, for a scalar LQ possessing the quantum numbers of the $S_{0,L}$ (which couples to e^-u). The domain excluded by the D0 experiment at the Tevatron [13] is also shown. For λ greater than ~ 0.06 , the H1 limits on scalar LQs extend considerably beyond the region excluded by the D0 experiment.

To summarise, a search for leptoquarks with fermion numbers $F = 2$ and $F = 0$ has been performed using all e^+p and e^-p data collected by H1 between 1994 and 2000. No signal has been observed and constraints on leptoquarks have been set, which extend beyond the domains excluded by other experiments at LEP and the Tevatron. For a coupling of electromagnetic strength, leptoquark masses below 275 – 325 GeV, depending on the leptoquark type, can be ruled out.

Acknowledgements

We are grateful to the HERA machine group whose outstanding efforts have made this experiment possible. We thank the engineers and technicians for their work in constructing and maintaining the H1 detector, our funding agencies for financial support, the DESY technical staff for continual assistance and the DESY directorate for support and for the hospitality which they extend to the non DESY members of the collaboration.

References

- [1] C. Adloff *et al.* [H1 Collaboration], Eur. Phys. J. C **11** (1999) 447 [Erratum-ibid. C **14** (1999) 553] [hep-ex/9907002].
- [2] C. Adloff *et al.* [H1 Collaboration], Phys. Lett. B. **523** (2001) 234 [hep-ex/0107038].
- [3] I. Abt *et al.* [H1 Collaboration], Nucl. Instrum. Meth. A **386** (1997) 310 and 348; R. D. Appuhn *et al.* [H1 SPACAL Group], Nucl. Instrum. Meth. A **386** (1997) 397.
- [4] C. Adloff *et al.* [H1 Collaboration], Eur. Phys. J. C **19** (2001) 269 [hep-ex/0012052].
- [5] DJANGO 6.2; G.A. Schuler and H. Spiesberger, Proc. of the Workshop Physics at HERA, W. Buchmüller and G. Ingelman (Editors), (October 1991, DESY-Hamburg) Vol. 3 p. 1419.
- [6] H. L. Lai *et al.* [CTEQ Collaboration], Eur. Phys. J. C **12** (2000) 375 [hep-ph/9903282].
- [7] W. Buchmüller, R. Rückl and D. Wyler, Phys. Lett. B **191** (1987) 442 [Erratum-ibid. B **448** (1999) 320].

⁵In the BRW model, $|\lambda_\nu| = |\lambda|$ for LQs coupling to both eq and νq since $\beta_\nu = \beta_e$. Here, in a generic LQ model, the effective coupling λ_ν at the LQ- ν - q vertex can be different from λ at the LQ- e - q vertex.

- [8] P. Bock, “Computation of confidence levels for exclusion or discovery of a signal with the method of fractional event counting” [hep-ex/0405072].
- [9] G. Abbiendi *et al.* [OPAL Collaboration], Eur. Phys. J. C **31** (2003) 281.
- [10] M. Botje, Eur. Phys. J. **C14** (2000) 285 [hep-ph/9912439];
<http://www.nikhef.nl/~h24/qcdnum/>.
- [11] A. Djouadi, T. Köhler, M. Spira and J. Tutas, Z. Phys. C **46** (1990) 679.
- [12] G. Abbiendi *et al.* [OPAL Collaboration], Eur. Phys. J. C **6** (1999) 1 [hep-ex/9808023];
M. Acciarri *et al.* [L3 Collaboration], Phys. Lett. B **486** (2000) 81 [hep-ex/0005028].
- [13] V. M. Abazov [D0 Collaboration], Phys. Rev. D **71** (2005) 071104 [hep-ex/0412029].
- [14] S. Chekanov *et al.* [ZEUS Collaboration], Phys. Rev. D **68** (2003) 052004 [hep-ex/0304008].
- [15] C. Adloff *et al.* [H1 Collaboration], Phys. Lett. B **568** (2003) 35 [hep-ex/0305015].
- [16] C. Adloff *et al.* [H1 Collaboration], Eur. Phys. J. C **30** (2003) 1 [hep-ex/0304003].
- [17] A. Aktas *et al.* [H1 Collaboration], Eur. Phys. J. C **36** (2004) 425 [hep-ex/0403027].

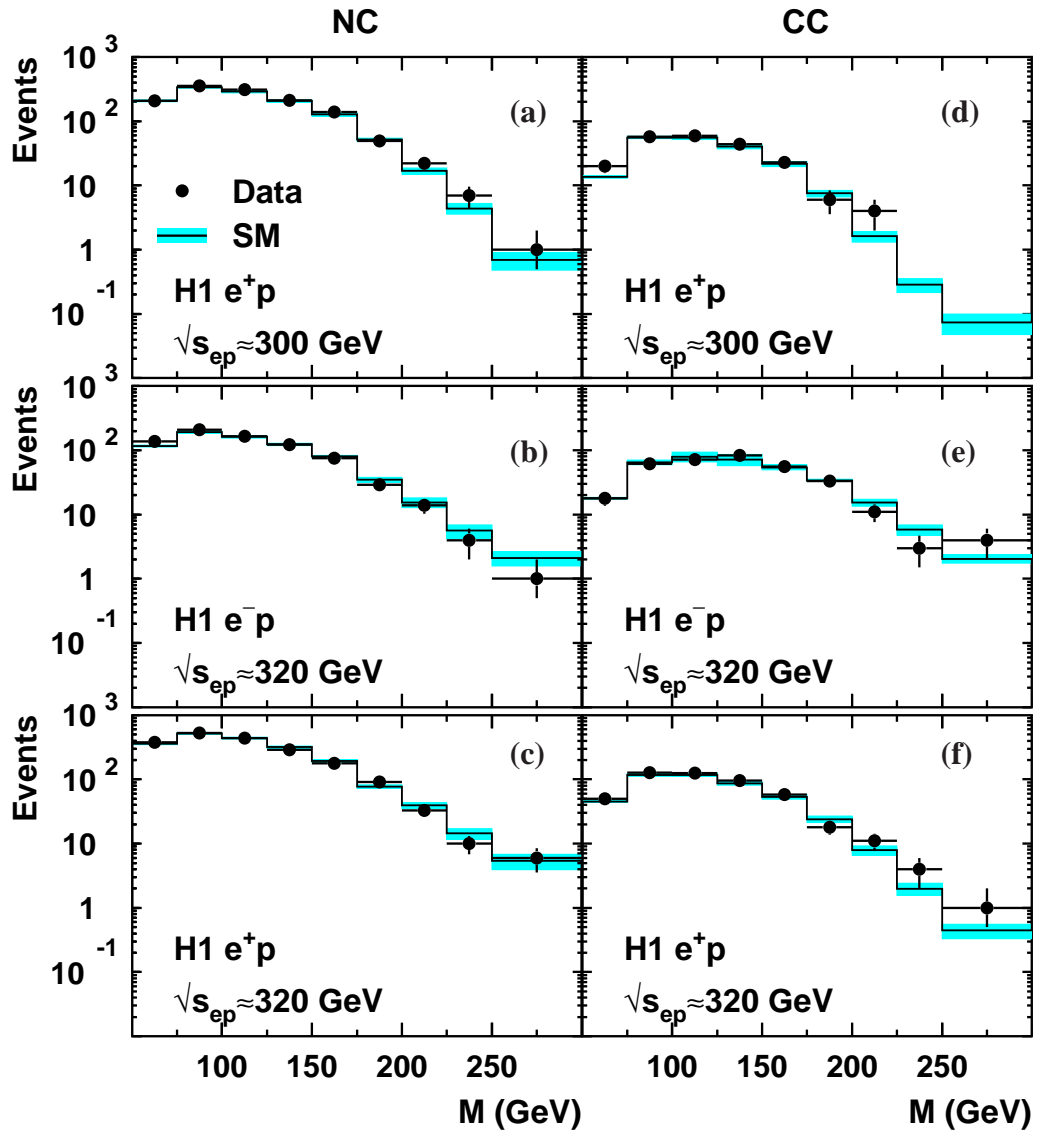


Figure 1: Mass spectra for the (a-c) neutral current (NC) and (d-f) charged current (CC) deep inelastic scattering selected events, together with the corresponding Standard Model (SM) expectations. The shaded bands indicate the $\pm 1\sigma$ uncertainty on the SM expectations.

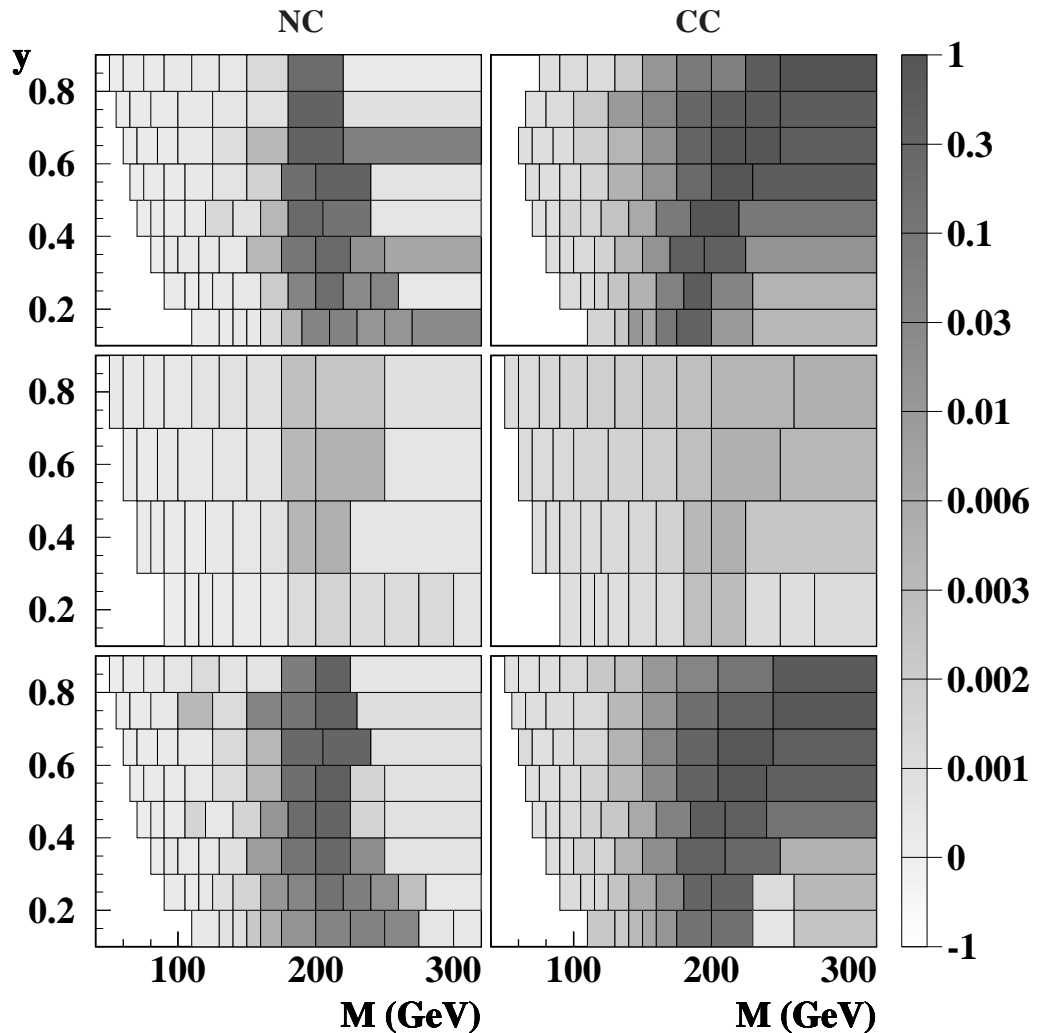


Figure 2: Binning used in the $M - y$ plane for the different data sets and weights calculated in these bins for a 200 GeV vector leptoquark with a coupling of 0.023 to e^+d and $\bar{\nu}u$. The left plots correspond to the neutral current (NC)-like decay channel whereas the right plots correspond to the charged current (CC)-like decay channel. The top, middle and bottom plots correspond to the 300 GeV e^+p , 320 GeV e^-p and 320 GeV e^+p data sets, respectively.

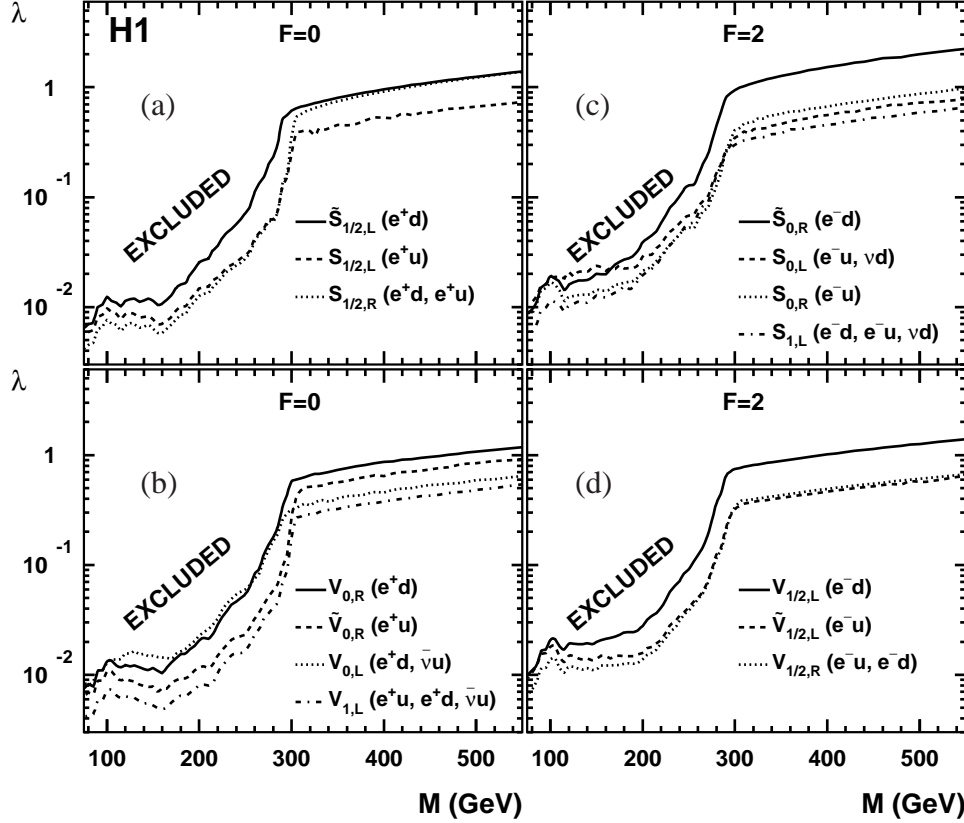


Figure 3: Exclusion limits for the 14 leptoquarks (LQs) described by the Buchmüller, Rückl and Wyler (BRW) model. The limits are expressed at 95% CL on the coupling λ as a function of the leptoquark mass for the (a) scalar LQs with $F = 0$, (b) vector LQs with $F = 0$, (c) scalar LQs with $F = 2$ and (d) vector LQs with $F = 2$. Domains above the curves are excluded. For each LQ type the pairs of Standard Model fermions coupling to it are indicated in brackets (charge conjugate states are not shown).

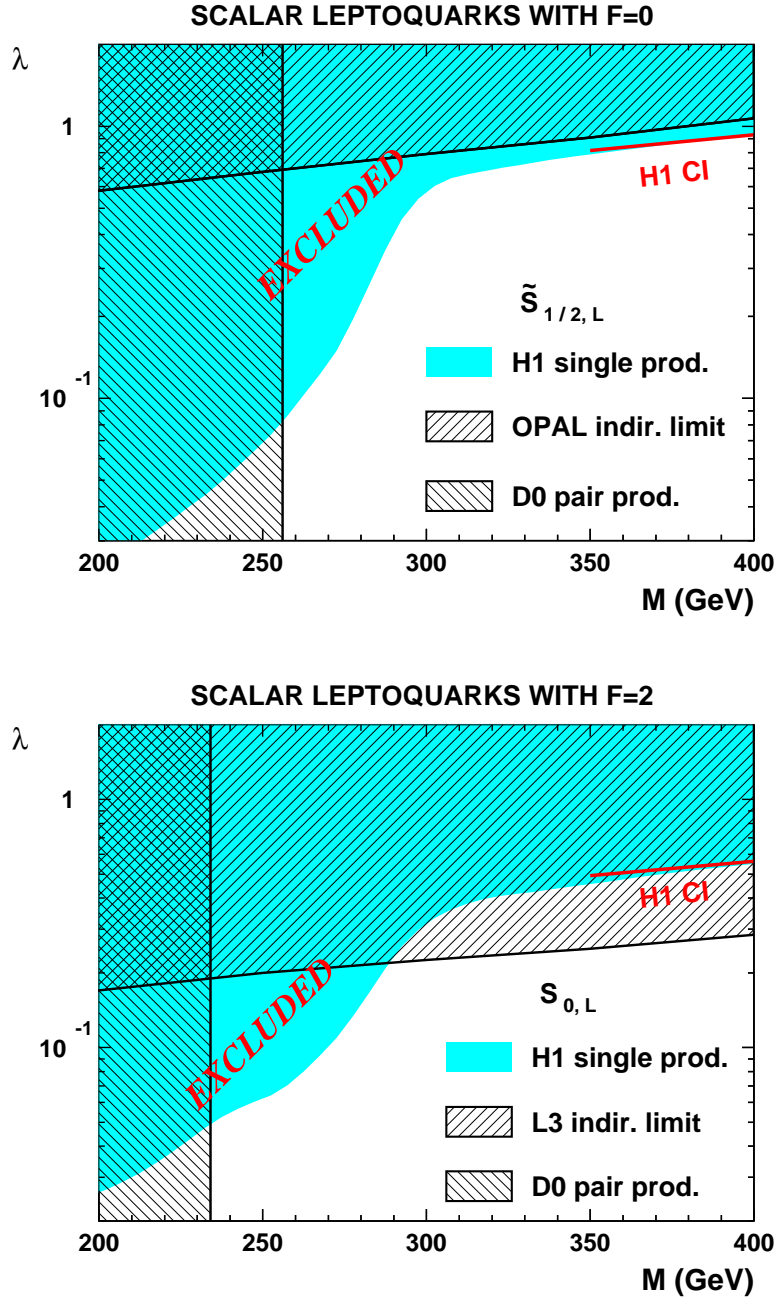


Figure 4: Exclusion limits at 95% CL on the coupling λ as a function of the leptoquark (LQ) mass for $\tilde{S}_{1/2,L}$ (top) and $S_{0,L}$ (bottom) in the framework of the BRW model. The direct D0 limits are independent of the coupling. For $\tilde{S}_{1/2,L}$ the indirect limit from OPAL is shown, whereas for $S_{0,L}$ the better indirect limit from L3 is shown. Constraints on LQs with masses above 350 GeV obtained from the H1 contact interaction (H1 CI) analysis [15] are also shown, in the rightmost part of the figures.

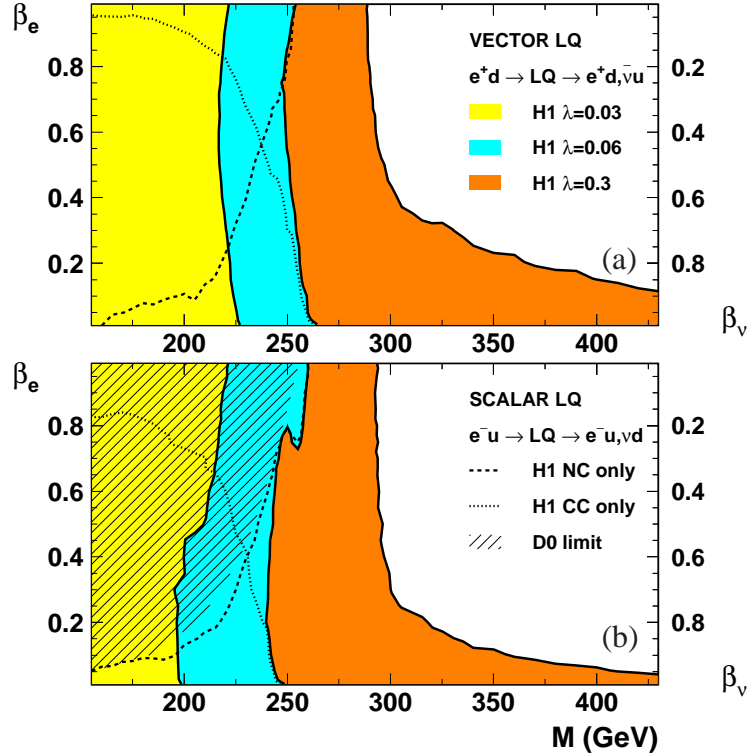


Figure 5: (a) Domains ruled out by the combination of the NC and CC analyses, for a vector LQ which couples to e^+d (with the quantum numbers of the $V_{0,L}$) and decaying only into eq and νq for three values of the coupling λ . (b) Same as for (a) but for a scalar LQ coupling to e^-u (with the quantum numbers of the $S_{0,L}$). The regions on the left of the full curves are excluded at 95% CL. For $\lambda = 0.06$, the part of the $\beta_e - M_{\text{LQ}}$ ($\beta_\nu - M_{\text{LQ}}$) plane on the left of the dashed (dotted) curve is excluded by the NC (CC) analysis alone. The branching ratios β_e and $\beta_\nu (= 1 - \beta_e)$ are shown on the left and right axes respectively. The excluded domains cover β_e values larger than 7.2×10^{-5} , 2.9×10^{-4} and 7.1×10^{-3} for $\lambda = 0.03$, 0.06 and 0.3 respectively. In (b) the hatched region represents the domain excluded by the D0 experiment. The D0 limits do not depend on the value of the coupling.